

e^+e^- production from pp reactions at BEVALAC energies

E. L. Bratkovskaya, W. Cassing, M. Effenberger and U. Mosel

Institute für Theoretische Physik, Universität Giessen, 35392 Giessen, Germany

Abstract

We have performed a detailed study of dilepton production from pp collisions including the subthreshold ρ production via baryonic resonances ($N(1520), N(1700)$) in addition to the conventional dilepton sources as π^0 , η , ω and Δ Dalitz decays and direct decays of vector mesons (ρ , ω). The role of baryonic resonances in ρ production from nucleon-nucleon collisions is studied in comparison to the DLS data which are well described.

PACS: 25.75.Dw, 13.30.Ce, 12.40.Yx

Keywords: particle and resonance production; leptonic and semileptonic decays; hadron mass models and calculations

I. INTRODUCTION

Dileptons are the most clear probes for an investigation of the early phases of high-energy heavy-ion collisions because they may leave the reaction volume essentially undistorted by final-state interactions. Dilepton spectra from heavy-ion collisions can provide information about the restoration of chiral symmetry and in-medium properties of hadrons (cf. Refs. [1–6]). According to QCD sum rules [2,5,7] as well as QCD inspired effective Lagrangian models [1,3,4,8], [9–14] the vector mesons (ρ , ω and ϕ) significantly change their properties with the nuclear density. In fact, the experimentally observed enhanced production of soft lepton pairs above known sources in nucleus-nucleus collisions at SPS energies [15,16] might be due to the in-medium modification of vector mesons [17–21].

Dileptons from heavy-ion collisions have also been measured by the DLS Collaboration [22,23] at BEVALAC energies, where a different temperature and density regime is probed. The first generation of DLS data [22], based on a limited data set, were consistent with the results from transport model calculations [24–27] including the conventional dileptons sources as pn bremsstrahlung, π^0 , η , ω and Δ Dalitz decay, direct decay of vector mesons and pion-pion annihilation, without incorporating any medium effects. A recent DLS measurement [23] including the full data set and an improved analysis shows an increase by about a factor of 5-7 in the cross section in comparison to Ref. [22] and the early theoretical predictions.

In Ref. [28] the in-medium rho spectral functions from Refs. [13,14] have been implemented in the HSD transport approach for ρ mesons produced in baryon-baryon, pion-baryon collisions as well as from $\pi\pi$ annihilation, and a factor of 2-3 enhancement has been

obtained compared to the case of a free ρ -spectral function. In Ref. [29] dropping vector meson masses and ω meson broadening were incorporated in the UrQMD transport model, which also showed an enhancement of the dilepton yield, however, the authors could not describe the new DLS data [23] as well. Another attempt to solve the DLS 'puzzle' has been performed recently in Ref. [30] where the dropping hadron mass scenario was considered together with the subthreshold ρ production in πN scattering via the baryonic resonance $N(1520)$ whose importance was pointed out in Refs. [14,31]. It was found that the enhancement of the dilepton spectra due to low mass ρ 's from the $N(1520)$ was not sufficient to match the DLS data. Thus, all in-medium scenarios that successfully have explained the dilepton enhancement at SPS energies failed to describe the new DLS dilepton data [23] from heavy-ion collisions.

Recently the DLS Collaboration has published dilepton data from elementary pp and pd collisions at 1-5 GeV [32]. This provides the possibility for an independent check of the elementary dilepton channels that enter as 'input' for transport calculations for heavy-ion reactions. Such an analysis has been carried out in Ref. [29] and it was shown that the dilepton invariant mass spectra from pp reactions at invariant masses from $0.3 \leq M \leq 0.6$ GeV are underestimated when incorporating only the π^0 , η , ω and Δ Dalitz decays and direct decays of vector mesons (ρ , ω).

Historically, the first calculations of dilepton production from hadronic bremsstrahlung and from the radiative decay of the Δ resonance in nucleon-nucleon collisions have been based on the soft-photon approximation [33] which can be considered as an upper limit [34]. Later on, the model has been refined and the dilepton production from elementary nucleon-nucleon reactions was studied within different microscopic models [35–39]. In Ref. [35,36] the dilepton yield was calculated at 1.0 and 2.1 GeV on the basis of the one-boson exchange model taking into account the dilepton production via Δ Dalitz decay and bremsstrahlung. It was found that the incorporation of the vector-meson form factor into the vertices with a Δ , N or π leads to a significant enhancement of the dilepton yield in the ρ mass region which substantially overestimated the pBe data [22] at that time. The same effect was found for pp dilepton radiation at 1 GeV in Ref. [39] based on a T-matrix approach. Furthermore, the dilepton yield from pp collisions at 4.9 GeV was calculated in Ref. [40] and it was found that 'inelastic' channels (final states with one or two pions in addition to the nucleons and dileptons) dominated the bremsstrahlung calculated within the soft-photon approximation.

In this article we perform a detailed study of dilepton production from pp collisions including the subthreshold ρ production via baryonic resonances ($N(1520)$, $N(1700)$) in addition to the conventional dilepton sources (π^0 , η , ω and Δ Dalitz decay, direct decay of vector mesons (ρ , ω)). We investigate the role of baryonic resonances in ρ production from nucleon-nucleon collisions on the basis of two independent resonance models from Peters et al. [14] and Manley et al. [41] in order to demonstrate the dominant theoretical uncertainties.

The paper is organized as follows: In Section 2 we discuss the ρ meson production via baryonic resonances in nucleon-nucleon collisions. In Section 3 we describe the elementary dilepton production channels while Section 4 contains a comparison with the DLS data. We close with a summary and discussion of open problems in Section 5.

II. ρ MESON PRODUCTION VIA BARYON RESONANCES IN NUCLEON-NUCLEON COLLISIONS

In the resonance model the total ρ production cross section from NN collisions via the $N(1520)$ can be calculated as

$$\sigma(s)^{NN \rightarrow RN \rightarrow \rho NN} = \int_{m_N+m_\pi}^{\sqrt{s}-m_N} d\mu \sigma(s, \mu)^{NN \rightarrow RN} \times \frac{2}{\pi} \frac{\mu^2}{(\mu^2 - m_R^2)^2 + (\mu \Gamma_{tot}^R(\mu))^2} \Gamma(\mu)^{R \rightarrow \rho N}. \quad (1)$$

The resonance production cross section $\sigma(s, \mu)^{NN \rightarrow RN}$ with good accuracy can be approximated by a constant matrix element (cf. Ref. [43]) and a flux factor, i.e.

$$\sigma(s, \mu)^{NN \rightarrow RN} = \frac{p_f}{sp_i} \frac{|\bar{\mathcal{M}}|^2}{16\pi}, \quad (2)$$

$$p_f = \frac{[(s - (\mu + m_N)^2)(s - (\mu - m_N)^2)]^{1/2}}{2\sqrt{s}}, \quad p_i = \frac{(s - 4m_N^2)^{1/2}}{2}. \quad (3)$$

The average matrix element $|\bar{\mathcal{M}}|$ for the $pp \rightarrow N^+(1520)p$ reaction has been obtained in Ref. [43] from a fit to π - and ρ - production channels; it was found to be $|\bar{\mathcal{M}}|^2 = 64\pi \text{ mb} \cdot \text{GeV}^2$.

According to Ref. [14] the partial decay width for the resonance decay $R \rightarrow \pi N$ is taken as

$$\Gamma_{R \rightarrow \pi N}(\mu) = \Gamma_0 \left(\frac{k_\pi(\mu)}{k_\pi(m_R)} \right)^{2l+1} \times \left(\frac{0.5^2 + k_\pi(m_R)^2}{0.5^2 + k_\pi(\mu)^2} \right)^{2l+1}, \quad (4)$$

$$k_\pi(\mu) = \frac{[(\mu^2 - (m_\pi + m_N)^2)(\mu^2 - (m_\pi - m_N)^2)]^{1/2}}{2\mu}, \quad (5)$$

with $l = 2$ and $\Gamma_0 = 0.066 \text{ GeV}$ for the $N(1520)$ resonance.

The total resonance decay width is assumed to be given by the sum of the pion- and rho-decay width (cf. page 116 of Ref. [14]):

$$\Gamma_{tot}^R = \Gamma_{R \rightarrow \pi N} + \Gamma_{R \rightarrow \rho N}, \quad (6)$$

where $\Gamma_{R \rightarrow \pi N}$ is defined according to Eq. (4) with $\Gamma_0 = 0.095 \text{ GeV}$ for $N(1520)$. The width $\Gamma_{R \rightarrow \rho N}$ at an invariant mass μ is calculated as

$$\Gamma_{R \rightarrow \rho N}(\mu) = \int_{2m_\pi}^{\mu - m_N} dM \frac{d\Gamma(\mu, M)^{R \rightarrow \rho N}}{dM}. \quad (7)$$

Furthermore, the partial decay width for the process $R \rightarrow \rho N$ is defined according to Ref. [14] in the following way:

$$\frac{d\Gamma(\mu, M)^{R \rightarrow \rho N}}{dM} = \left(\frac{f_{RN\rho}}{m_\rho} \right)^2 \frac{1}{\pi} M \frac{m_N}{\mu} k_\rho (2\omega_\rho^2 + M^2) A(M) F(k_\rho^2), \quad (8)$$

where μ is the resonance mass, $f_{RN\rho}$ is the coupling constant ($f_{N(1520)N\rho} = 7$ [14]), k_ρ denotes the three-momentum of the ρ meson in the R resonance rest frame,

$$k_\rho = \frac{[(\mu - (M + m_N)^2)(\mu - (M - m_N)^2)]^{1/2}}{2\mu}, \quad (9)$$

while $\omega_\rho^2 = k_\rho^2 + M^2$ is the ρ energy. In Eq. (8) $A(M)$ is the vacuum ρ spectral function, i.e. a Breit-Wigner distribution

$$A(M) = \frac{1}{\pi} \frac{m_\rho \Gamma_{tot}^\rho(M)}{(M^2 - m_\rho^2)^2 + (m_\rho \Gamma_{tot}^\rho(M))^2}. \quad (10)$$

Moreover, $F(\mathbf{k}_\rho^2)$ is a monopole form factor

$$F(\mathbf{k}_\rho^2) = \frac{\Lambda^2}{\Lambda^2 + \mathbf{k}_\rho^2}, \quad \Lambda = 1.5 \text{ GeV}, \quad (11)$$

while the total ρ width is

$$\Gamma_{tot}^\rho(M) = \Gamma_{\rho \rightarrow \pi\pi}(m_\rho) \left(\frac{m_\rho}{M}\right) \left(\frac{k_\pi(M)}{k_\pi(m_\rho)}\right)^3. \quad (12)$$

The ρ production cross section from pp collisions via $N(1520)$ calculated according to Eqs. (1)–(3) with the resonance widths from Peters et al. [14] is shown in Fig. 1 as a solid line. The dot-dashed line presents the result within the analysis from Manley et al. [41]. The dashed line, furthermore, indicates the parametrization for the inclusive ρ production from Ref. [44] integrated over the kinematically allowed range of invariant mass of the ρ spectral function. The full circles are the experimental data [42] for the exclusive ρ production whereas the open square corresponds to the inclusive data point at high \sqrt{s} .

As seen from Fig. 1 at $\sqrt{s} > 2m_N + m_\rho$ the relative contribution of ρ 's stemming from the $N(1520)$ is small compared to the total inclusive ρ production cross section. However, closer to threshold the $N(1520)$ plays a dominant role in ρ production with low invariant masses since the cross section is dominated by the resonance amplitude.

In our analysis we also include the $N(1700)$ resonance in a similar way as the $N(1520)$ using again the parameters from Peters et al. [14]. We discard higher resonances, e.g. $N(1720)$, $N(1905)$, because already the $N(1700)$ plays only a minor role in the results to be discussed in this study.

III. ELEMENTARY DILEPTON PRODUCTION CHANNELS

In our analysis we calculate dilepton production by taking into account the contributions from the following channels:

$$pp \rightarrow N(1520)p, \quad N(1520) \rightarrow \rho^0 p \rightarrow e^+ e^- p, \quad (13)$$

$$pp \rightarrow N(1700)p, \quad N(1700) \rightarrow \rho^0 p \rightarrow e^+ e^- p, \quad (14)$$

$$pp \rightarrow \Delta N, \quad \Delta \rightarrow N e^+ e^-, \quad (15)$$

$$pp \rightarrow \eta X, \eta \rightarrow \gamma e^+ e^-, \quad (16)$$

$$pp \rightarrow \omega X, \omega \rightarrow \pi^0 e^+ e^-, \quad (17)$$

$$pp \rightarrow \pi^0 X, \pi^0 \rightarrow \gamma e^+ e^-, \quad (18)$$

$$pp \rightarrow \rho^0 X, \rho \rightarrow e^+ e^-, \quad (19)$$

$$pp \rightarrow \omega X, \omega \rightarrow e^+ e^-. \quad (20)$$

For the processes (13)–(20) we use the assumption that the amplitude can be factorized into a meson or resonance production and dilepton decay part, i.e. we cut the diagram as illustrated in Fig. 2, e.g., for the process (15) with an intermediate Δ resonance. This assumption provides not only a significant simplification, which is necessary for applications in transport calculations [25,45], but also allows to take into account the ‘inelasticity’ from many-particle production channels which become dominant at high energy. Note that the factorization ansatz holds (also in case of broad resonances) when integrating over the final relative angle between the dilepton and a proton; it becomes questionable only for the multi-differential dilepton cross sections. Since we will compare to practically angle integrated data (see below), this approximation should be justified for our present study.

We discard the pp bremsstrahlung from the nucleon pole since the microscopic OBE calculations [36,38,39] have shown that at 1.0 GeV the pp bremsstrahlung is smaller than the Δ Dalitz decay contribution by a factor of 2-3. At this energy also the interference between nucleon and Δ -pole terms is negligible. At high energies, where this interference becomes important [36], the overall contribution from these channels is negligible (see below).

A. Dilepton production through the $N(1520)$ resonance

Within the above assumptions the dilepton cross section from NN collisions via the $N(1520)$ can be factorized as

$$\frac{d\sigma(s, M)}{dM}^{NN \rightarrow RN \rightarrow \rho^0 NN \rightarrow e^+ e^- NN} = \frac{d\sigma(s, M)}{dM}^{NN \rightarrow \rho NN} \frac{\Gamma_{\rho \rightarrow e^+ e^-}(M)}{\Gamma_{tot}^\rho(M)}, \quad (21)$$

where the differential ρ production cross section with mass M is

$$\begin{aligned} \frac{d\sigma(s, M)}{dM}^{NN \rightarrow \rho NN} &= \int_{m_N + m_\pi}^{\sqrt{s} - m_N} d\mu \sigma(s, \mu)^{NN \rightarrow RN} \\ &\times \frac{2}{\pi} \frac{\mu^2}{(\mu^2 - m_R^2)^2 + (\mu \Gamma_{tot}^R(\mu))^2} \frac{d\Gamma(\mu, M)^{R \rightarrow \rho N}}{dM}. \end{aligned} \quad (22)$$

The partial decay width $d\Gamma(\mu, M)^{R \rightarrow \rho N}/dM$ is given by Eq. (8), the total width Γ_{tot}^R is defined according Eq. (6) while the ρ width is taken according to Eq. (12).

In (21), $\Gamma_{\rho \rightarrow e^+ e^-}(M)$ is the dilepton decay width of a neutral ρ meson of mass M which in line with the vector dominance model is taken as

$$\Gamma_{\rho \rightarrow e^+ e^-}(M) = C_\rho \frac{m_\rho^4}{M^3} \quad (23)$$

with $C_\rho = 8.8 \times 10^{-6}$.

To compare with the experimental data of the DLS collaboration one has to use the appropriate experimental filter, which is a function of the dilepton invariant mass M , transverse momentum q_T and rapidity y_{lab} in the laboratory frame – $F(M, q_T, y_{lab})$. For that purpose we explicitly simulate the dileptons by Monte-Carlo: first, we produce the resonance $N(1520)$ isotropically in the center-of-mass frame of the pp collision with momentum p_f (3). In the same way we create the ρ mesons in the $N(1520)$ rest frame with momentum k_ρ (9) and perform a Lorentz transformation to the laboratory frame, where the filter $F(M, q_T, y_{lab})$ is applied. A similar procedure has been used for all other channels. We note that we applied the DLS acceptance filter (version 4.1).

In Fig. 3 we show the dilepton invariant mass spectra from the channel $pp \rightarrow N(1520)p \rightarrow \rho^0 pp \rightarrow e^+e^-pp$ at 1.61 GeV calculated without experimental filter. The solid line indicates the result calculated according to Peters et al. [14], while the dashed line corresponds to the resonance analysis of Manley et al. [41]. The dilepton yield for the parameters from [14] is by a factor of 2 larger than that from Manley et al. [41] due to the differences in the resonance parameters and parametrizations for the widths. Our future results for dileptons via $N(1520)$ are based on Ref. [14], however, one has to keep in mind the theoretical uncertainties indicated here. This also holds for the uncertainties induced by the neglect of interference terms between the different diagrams. Whereas the latter vanish for diagrams with different quantum numbers in the intermediate state after integration over the relative angle between the dilepton and a final proton, they might be essential in some regions of phase space for multi-differential cross sections. However, when integrating over a wide region of phase space (see below) the uncertainty due to the interference of diagrams should be much smaller than the uncertainty of the factor of 2 stemming from the different resonance model parameters.

B. Dalitz decays

The process $pp \rightarrow \Delta N \rightarrow NN e^+e^-$ is treated as a two step process – the Δ production from the pp interaction ($pp \rightarrow \Delta N$) and the Δ Dalitz decay ($\Delta \rightarrow Ne^+e^-$) – cf. Fig. 2. For the Δ production below 2.1 GeV we adopt the differential cross section from Refs. [25,43], where the Δ resonances are created with a mass according to a Breit-Wigner distribution with a momentum dependent width. At the higher energies we obtain the Δ cross section from the LUND model [49]. Also the π^0 production has been performed via the Δ resonance excitation and decay in line with Refs. [25,43].

For the Δ Dalitz-decay we use the $N\Delta\gamma$ vertex as in Ref. [25]

$$\mathcal{L}_{int} = eA^\mu \bar{\Psi}_\Delta^\beta \Gamma_{\beta\mu} \Psi_N, \quad (24)$$

where

$$\begin{aligned} \Gamma_{\beta\mu} &= g f \eta_{\beta\mu}, \\ f &= -\frac{3}{2} \frac{m_\Delta + m_N}{m_N ((m_\Delta + m_N)^2 - M^2)}, \\ \eta_{\beta\mu} &= -M \chi_{\beta\mu}^1 + \chi_{\beta\mu}^2 + 0.5 \chi_{\beta\mu}^3, \end{aligned} \quad (25)$$

$$\begin{aligned}
\chi_{\beta\mu}^1 &= (q_\beta\gamma_\mu - q_\nu\gamma^\nu g_{\beta\mu})\gamma_5, \\
\chi_{\beta\mu}^2 &= (q_\beta\bar{P}_\mu - q_\nu\bar{P}^\nu g_{\beta\mu})\gamma_5, \\
\chi_{\beta\mu}^3 &= (q_\beta q_\mu - M^2 g_{\beta\mu})\gamma_5, \\
\bar{P} &= \frac{1}{2}(p_\Delta + p_N),
\end{aligned}$$

and $g = 5.44$ is the coupling constant fitted to the radiative decay width $\Gamma_0(0) = 0.72$ MeV.

The processes (16),(17),(18) are calculated in a similar way as the Δ Dalitz decay (15), i.e. first η , ω or π^0 mesons are produced in pp interactions and then their Dalitz decay $\eta \rightarrow \gamma e^+ e^-$, $\omega \rightarrow \pi^0 e^+ e^-$ and $\pi^0 \rightarrow \gamma e^+ e^-$ is simulated by Monte-Carlo.

For the η meson production cross section we adopt the parametrization from Refs. [25,46] in line with the data from the WASA collaboration [47]. The η Dalitz-decay to $\gamma e^+ e^-$ is given by [48]:

$$\begin{aligned}
\frac{d\Gamma_{\eta \rightarrow \gamma e^+ e^-}}{dM} &= \frac{4\alpha}{3\pi} \frac{\Gamma_{\eta \rightarrow 2\gamma}}{M} \left(1 - \frac{4m_e^2}{M^2}\right)^{1/2} \left(1 + 2\frac{m_e^2}{M^2}\right) \\
&\quad \times \left(1 - \frac{M^2}{m_\eta^2}\right)^3 |F_{\eta \rightarrow \gamma e^+ e^-}(M)|^2,
\end{aligned} \tag{26}$$

where the form factor is parametrized in the pole approximation as

$$F_{\eta \rightarrow \gamma e^+ e^-}(M) = \left(1 - \frac{M^2}{\Lambda_\eta^2}\right)^{-1} \tag{27}$$

with the cut-off parameter $\Lambda_\eta \simeq 0.72$ GeV.

The π^0 Dalitz decay is calculated in a similar way using the form factor from Ref. [48], i.e.

$$F_{\pi^0 \rightarrow \gamma e^+ e^-}(M) = \left(1 + B_{\pi^0} M^2\right), \tag{28}$$

with $B_{\pi^0} = 5.5$ GeV⁻².

Similarly, the ω Dalitz-decay is [48]

$$\begin{aligned}
\frac{d\Gamma_{\omega \rightarrow \pi^0 e^+ e^-}}{dM} &= \frac{2\alpha}{3\pi} \frac{\Gamma_{\omega \rightarrow \pi^0 \gamma}}{M} \left(1 - \frac{4m_e^2}{M^2}\right)^{1/2} \left(1 + 2\frac{m_e^2}{M^2}\right) \\
&\quad \times \left[\left(1 + \frac{M^2}{m_\omega^2 - m_\pi^2}\right)^2 - \frac{4m_\omega^2 M^2}{(m_\omega^2 - m_\pi^2)^2} \right]^{3/2} |F_{\omega \rightarrow \pi^0 e^+ e^-}(M)|^2,
\end{aligned} \tag{29}$$

where the form factor squared is parametrized as [48,19]

$$|F_{\omega \rightarrow \pi^0 e^+ e^-}(M)|^2 = \frac{\Lambda_\omega^4}{(\Lambda_\omega^2 - M^2)^2 + \Lambda_\omega^2 \Gamma_\omega^2} \tag{30}$$

with

$$\Lambda_\omega = 0.65 \text{ GeV}, \quad \Gamma_\omega = 75 \text{ MeV}.$$

C. Vector meson decay

In a first step we calculate the production of vector mesons in pp collisions and as a second step the direct decay of vector mesons to dileptons. The vector meson production in pp interactions is evaluated in the following way: close to threshold, i.e. $T_{kin} \leq 2.1$ GeV, we use the inclusive mass differential parametrization for the ρ (dashed line in Fig. 1) and ω production from pp collisions. The mass of the vector meson M is distributed according to the Breit-Wigner form:

$$f(M) = N_V \frac{2}{\pi} \frac{M m_V \Gamma_{tot}^V}{(M^2 - m_V^2)^2 + (m_V \Gamma_{tot}^V)^2}, \quad (31)$$

while N_V guarantees normalization to unity, i.e. $\int f(M) dM = 1$. The total ρ meson width Γ_{tot}^ρ is defined according to Eq. (12). For the narrow ω meson we use a constant width $\Gamma_{tot}^\omega = 0.00841$ GeV. The ρ momentum is simulated according to the 3-body phase space since we are close to the ρ production threshold.

The vector meson decay to dileptons then is calculated according to the branching ratio,

$$\text{Br}(M) = \frac{\Gamma_{V \rightarrow e^+e^-}(M)}{\Gamma_{tot}^V(M)}, \quad (32)$$

where $\Gamma_{V \rightarrow e^+e^-}(M)$ is given by Eq. (23) with $C_\omega = 1.344 \times 10^{-6}$ for ω mesons.

D. Dilepton production at 4.9 GeV

With increasing energy, i.e. at 4.9 GeV, multiple particle production channels become dominant. In order to take into account correctly the many-body phase space, the FRITIOF event generator version 7.02 based on the LUND string fragmentation model [49] has been used for $\eta, \omega, \rho, \Delta, \pi^0$ production. The FRITIOF model gives a good description of the experimental data for meson production in NN collisions (for details see, e.g., Ref. [45]). The vector mesons as well as Δ resonances produced by the FRITIOF generator acquire masses according to the Breit-Wigner distribution while taking into account the proper available phase space. The dilepton decay of $\eta, \omega, \rho, \Delta, \pi^0$ is then treated in the same way as described above.

IV. COMPARISON TO THE DLS DATA

A. Differential mass spectra

In Fig. 4 we present the calculated dilepton invariant mass spectra $d\sigma/dM$ for pp collisions from 1.0 – 4.9 GeV including the final mass resolution and filter $F(M, q_T, y_{lab})$ from the DLS collaboration in comparison to the DLS data [32]. The thin lines indicate the individual contributions from the different production channels; *i.e.* starting from low M : Dalitz decay $\pi^0 \rightarrow \gamma e^+e^-$ (short dashed line), $\eta \rightarrow \gamma e^+e^-$ (dotted line), $\Delta \rightarrow N e^+e^-$ (dashed line), $\omega \rightarrow \pi^0 e^+e^-$ (dot-dot-dashed line), $N(1520) \rightarrow N e^+e^-$ (dot-dashed line); $N(1700) \rightarrow$

$N e^+ e^-$ (dotted line); for $M \approx 0.7$ GeV: $\omega \rightarrow e^+ e^-$ (dot-dot-dashed line), $\rho^0 \rightarrow e^+ e^-$ (short dashed line). The full solid line represents the sum of all sources considered here.

Whereas at 1.04 GeV the dileptons stem practically all from π^0 and Δ Dalitz decays, η and $N(1520)$ Dalitz decays become more important at 1.27 GeV, which is just above the η production threshold. The contribution from the $N(1520)$ is most prominent at 1.61 GeV and much larger than the other channels for $M \geq 0.5$ GeV, whereas the η decay dominates already at 1.85 GeV. Note that the η cross section in pp collisions is well known experimentally [50] as well as the π^0 and Δ resonance yields. The contribution of the $N(1520)$ thus is necessary for a proper description of the pp data especially at 1.61 GeV. The contribution of the $N(1700)$ is always below the $N(1520)$ and is practically not seen.

At 2.1 GeV the direct decays of ρ and ω mesons become dominant for $M \geq 0.65$ GeV. However, even at this higher energy for $M \simeq 0.6$ GeV the contribution from the $N(1520)$ is still seen. At 4.9 GeV the dilepton yield is dominated by the η Dalitz decay and direct decays of ρ and ω mesons. The ρ spectrum is enhanced towards low M due to the limited phase space and strong mass dependence (M^{-3}) of the dilepton decay width (23) in line with the vector dominance model.

B. Rapidity spectra

In Figs. 5 and 6 we show the laboratory rapidity spectra for dileptons from pp collisions at 1.0 – 4.9 GeV, imposing as in the data a low mass limit of 0.15 GeV (Fig. 5) and 0.25 GeV (Fig. 6) in comparison to the DLS data [32]. The experimental low mass limits applied here allow to exclude the contribution of the π^0 Dalitz decay and partly suppress (for the 0.25 GeV cut) the contributions from η and Δ Dalitz decays (cf. Fig. 4).

Both at 1.04 and 1.27 GeV the Δ Dalitz decay is dominant (Figs. 5, 6). At 1.61 GeV with a 0.25 GeV lower mass limit the $N(1520)$ contribution becomes visible (Fig. 6). However, at 1.85 – 4.9 GeV basically the η Dalitz decay contributes to the rapidity spectra since this channel has the largest differential cross section $d\sigma/dM$ (cf. Fig. 4). Note again, that the η cross section from pp collisions is well known experimentally which provides a valuable control of independent dilepton data.

C. Excitation function

The excitation function, i.e. the integrated dilepton cross section for masses above 0.15 GeV, is shown in Fig. 7 in comparison to the DLS data [32] (full circles). The experimental total cross section at 1.0 GeV ($Q = \sqrt{s} - 2m_p = 0.46$ GeV) is larger than at 1.27 GeV ($Q = 0.55$ GeV). We underestimate $\sigma(s)$ at 1.0 GeV, but stay on the upper level of error bars at 1.27 GeV, which is consistent with the dilepton mass spectra of Fig. 4. Thus we get a monotonous increase of the total cross section with energy because of the increase of the available phase space and new channels opening up. The discrepancy with the DLS data at 1.0 – 1.27 GeV might be due to experimental uncertainties, since the excitation function for pd collisions measured by the DLS collaboration indicates also a monotonous increase [32].

V. SUMMARY

We have studied dilepton production from pp collisions at 1.0 – 4.9 GeV in comparison to the data of the DLS Collaboration which provide sensible constraints on the different individual production channels. In addition to the conventional dilepton sources as π^0 , η , ω and Δ Dalitz decays and direct decays of vector mesons (ρ , ω) we have included the subthreshold ρ production via baryonic resonances ($N(1520)$, $N(1700)$). It has been shown that the baryonic resonances play an essential role in the low mass ρ production in pion-nucleon and nucleon-nucleon collisions below the experimentally seen threshold. The contribution from the baryonic resonances, in particular $N(1520)$, can be seen in the invariant mass dilepton spectra, especially at 1.61 GeV, and in the rapidity distributions when imposing low mass cuts in order to suppress the contributions from π^0 , η and Δ Dalitz decays.

Our results for the differential mass spectra including the conventional sources mentioned above are in general agreement with the calculations from Ref. [29]. The remaining differences might be attributed to different parametrizations for the meson production cross sections used since the existing experimental data so far allow for different fits within the error bars.

It has been found that the DLS data for pp collisions – their invariant mass spectra, laboratory rapidity distributions and total dilepton production cross section – can be well described including all channels mentioned above in an incoherent way. This might indicate that interference effects between different channels are hardly visible where integrating over a wide region in phase space. Our analysis has shown that the 'input' used in transport calculations for heavy-ion and proton-nucleus collisions [19–21,28,30,45] is in agreement with the DLS pp data.

The 'puzzle' that the DLS heavy-ion data cannot be reproduced within such calculations thus requires future investigations or/and new independent experimental data as expected in future from the HADES collaboration. We stress that dilepton data should be taken from pp , pd , pA , AA as well as πp , πd and πA collisions under the same experimental conditions to allow for a sensitive test of in-medium properties of the vector mesons.

ACKNOWLEDGMENTS

The authors are grateful for valuable discussions with C. Gale and C. M. Ko. This work has been supported by GSI, BMBF and DFG.

REFERENCES

- [1] G.E. Brown and M. Rho, Phys. Rev. Lett. 66 (1991) 2720.
- [2] T. Hatsuda and S. Lee, Phys. Rev. C 46 (1992) R34.
- [3] C.M. Shakin and W.-D. Sun, Phys. Rev. C 49 (1994) 1185.
- [4] F. Klingl and W. Weise, Nucl. Phys. A 606 (1996) 329; F. Klingl, N. Kaiser and W. Weise, Nucl. Phys. A 624 (1997) 527.
- [5] M. Asakawa and C.M. Ko, Phys. Rev. C 48 (1993) R526.
- [6] U. Mosel, Ann. Rev. Nucl. Part. Sci. 41 (1991) 29.
- [7] S. Leupold, W. Peters and U. Mosel, Nucl. Phys. A 628 (1998) 311.
- [8] M. Herrmann, B. Friman, and W. Nörenberg, Nucl. Phys. A 560 (1993) 411.
- [9] M. Asakawa, C. M. Ko, P. Lévai, and X. J. Qiu, Phys. Rev. C 46 (1992) R1159.
- [10] G. Chanfray and P. Schuck, Nucl. Phys. A 545 (1992) 271c.
- [11] R. Rapp, G. Chanfray, and J. Wambach, Phys. Rev. Lett. 76 (1996) 368.
- [12] B. Friman and H. J. Pirner, Nucl. Phys. A 617 (1997) 496.
- [13] R. Rapp, G. Chanfray and J. Wambach, Nucl. Phys. A 617 (1997) 472.
- [14] W. Peters, M. Post, H. Lenske, S. Leupold, and U. Mosel, Nucl. Phys. A 632 (1998) 109.
- [15] G. Agakichiev et al., Phys. Rev. Lett. 75 (1995) 1272; Th. Ullrich et al., Nucl. Phys. A 610 (1996) 317c; A. Drees, Nucl. Phys. A 610 (1996) 536c.
- [16] M. A. Mazzoni, Nucl. Phys. A 566 (1994) 95c; M. Masera, Nucl. Phys. A 590 (1995) 93c; T. Åkesson et al., Z. Phys. C 68 (1995) 47.
- [17] G. Q. Li, C. M. Ko, and G. E. Brown, Phys. Rev. Lett. 75 (1995) 4007.
- [18] C. M. Ko, G. Q. Li, G. E. Brown, and H. Sorge, Nucl. Phys. A 610 (1996) 342c.
- [19] W. Cassing, W. Ehehalt, and C. M. Ko, Phys. Lett. B 363 (1995) 35; W. Cassing, W. Ehehalt, and I. Kralik, Phys. Lett. B 377 (1996) 5.
- [20] E. L. Bratkovskaya and W. Cassing, Nucl. Phys. A 619 (1997) 413.
- [21] W. Cassing, E. L. Bratkovskaya, R. Rapp, and J. Wambach, Phys. Rev. C 57 (1998) 916.
- [22] G. Roche et al., Phys. Rev. Lett. 61 (1988) 1069; C. Naudet et al., Phys. Rev. Lett. 62 (1989) 2652; G. Roche et al., Phys. Lett. B 226 (1989) 228.
- [23] R.J. Porter et al., Phys. Rev. Lett. 79 (1997) 1229.
- [24] L. Xiong, Z. G. Wu, C. M. Ko, and J. Q. Wu, Nucl. Phys. A 512 (1990) 772.
- [25] Gy. Wolf, G. Batko, W. Cassing, U. Mosel, K. Niita, and M. Schäfer, Nucl. Phys. A 517 (1990) 615; Gy. Wolf, W. Cassing and U. Mosel, Nucl. Phys. A 552 (1993) 549.
- [26] K.K. Gudima, A.I. Titov and V.D. Toneev, Sov. Jour. of Nucl. Phys. 55 (1992) 1715.
- [27] E. L. Bratkovskaya, W. Cassing and U. Mosel, Phys. Lett. B 376 (1996) 12.
- [28] E. L. Bratkovskaya, W. Cassing, R. Rapp, and J. Wambach, Nucl. Phys. A 634 (1998) 168.
- [29] C. Ernst, S. A. Bass, M. Belkacem, H. Stöcker, and W. Greiner, Phys. Rev. C 58 (1998) 447.
- [30] E.L. Bratkovskaya and C.M. Ko, Phys. Lett. B 445 (1999) 265.
- [31] G. E. Brown, G. Q. Li, R. Rapp, M. Rho, and J. Wambach, Acta Phys. Polon. B 29 (1998) 2309.
- [32] W.K. Wilson et al., Phys. Rev. C 57 (1998) 1865.
- [33] C. Gale and J. Kapusta, Phys. Rev. C 35 (1987) 2107; C 40 (1987) 2397.

- [34] P. Lichard, Phys. Rev. D 51 (1995) 6017.
- [35] M. Schäfer, T. Biro, W. Cassing, and U. Mosel, Phys. Lett. B 221 (1989) 1.
- [36] M. Schäfer, H.C. Dönges, A. Engel and U. Mosel, Nucl. Phys. A 575 (1994) 429.
- [37] K. Haglin, Ann. Phys. 212 (1991) 84.
- [38] A.I. Titov, B. Kämpfer and E.L. Bratkovskaya, Phys. Rev. C 51 (1995) 227.
- [39] F. de Jong and U. Mosel, Phys. Lett. B 379 (1996) 45; B 392 (1997) 273.
- [40] K. Haglin and C. Gale, Phys. Rev. C 49 (1994) 401.
- [41] D.M. Manley and E.M. Saleski, Phys. Rev. D 45 (1992) 4002.
- [42] Landolt-Börnstein, New Series, ed. H. Schopper, I/12 (1988).
- [43] S. Teis, W. Cassing, M. Effenberger, A. Hombach, U. Mosel, and Gy. Wolf, Z. Phys. A 356 (1997) 421; Z. Phys. A 359 (1997) 297.
- [44] A. Sibirtsev, W. Cassing and U. Mosel, Z. Phys. A 358 (1997) 357.
- [45] W. Cassing and E. L. Bratkovskaya, Phys. Rep. 308 (1999) 65.
- [46] T. Vetter, A. Engel, T. Biro and U. Mosel, Phys. Lett. B 263 (1991) 153.
- [47] H. Calén et al., Phys. Lett. B 366 (1996) 39; Phys. Rev. Lett. 79 (1997) 2642; 80 (1998) 2069.
- [48] L. G. Landsberg, Phys. Rep. 128 (1985) 301.
- [49] B. Anderson, G. Gustafson and Hong Pi, Z. Phys. C 57 (1993) 485.
- [50] E. Chiavassa et al., Phys. Lett. B 322 (1994) 270; B 337 (1994) 192.

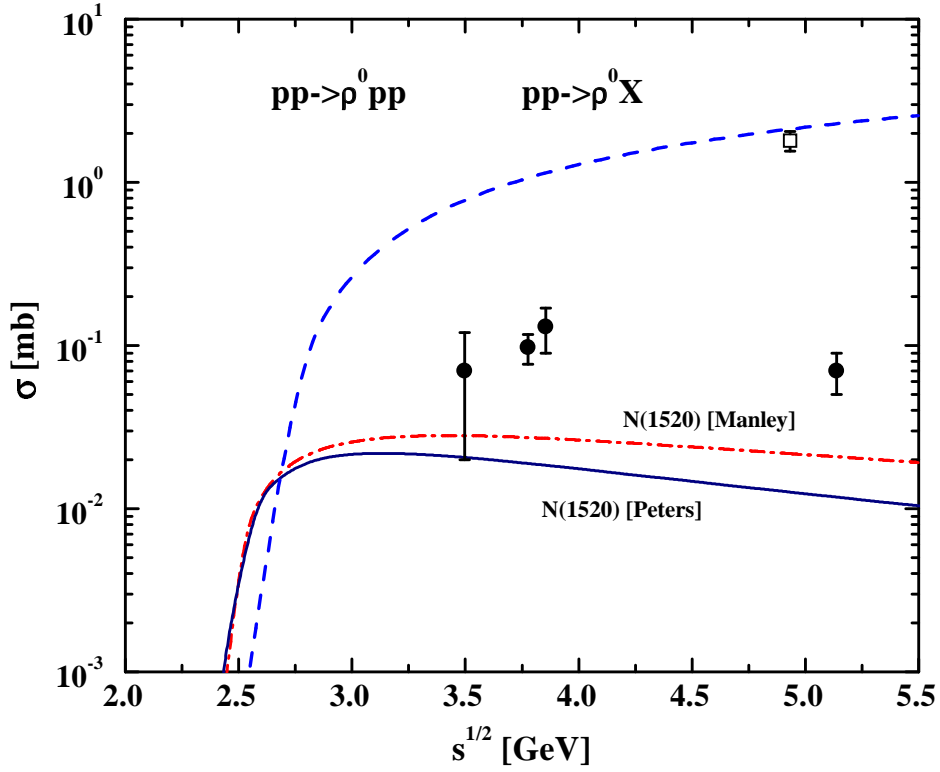


FIG. 1. The ρ production cross section from the $pp \rightarrow N(1520)p \rightarrow \rho^0 pp$ channel calculated according to the resonance models from Ref. [14] (full line) and from Ref. [41] (dot-dashed line) as a function of the invariant energy \sqrt{s} . The dashed line indicates the parametrization for inclusive ρ production in pp collisions from Ref. [44] integrated over the kinematically allowed range of invariant mass of the ρ spectral function. The full circles are the experimental data [42] for the exclusive ρ production whereas the open square corresponds to the inclusive data point at high \sqrt{s} .

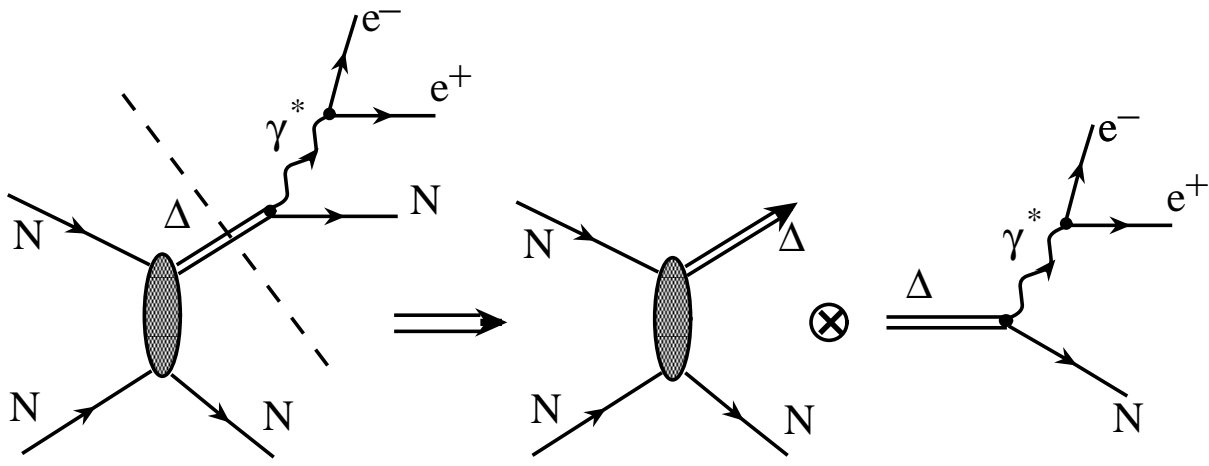


FIG. 2. Factorization of the diagram for the process (15) with an intermediate Δ .

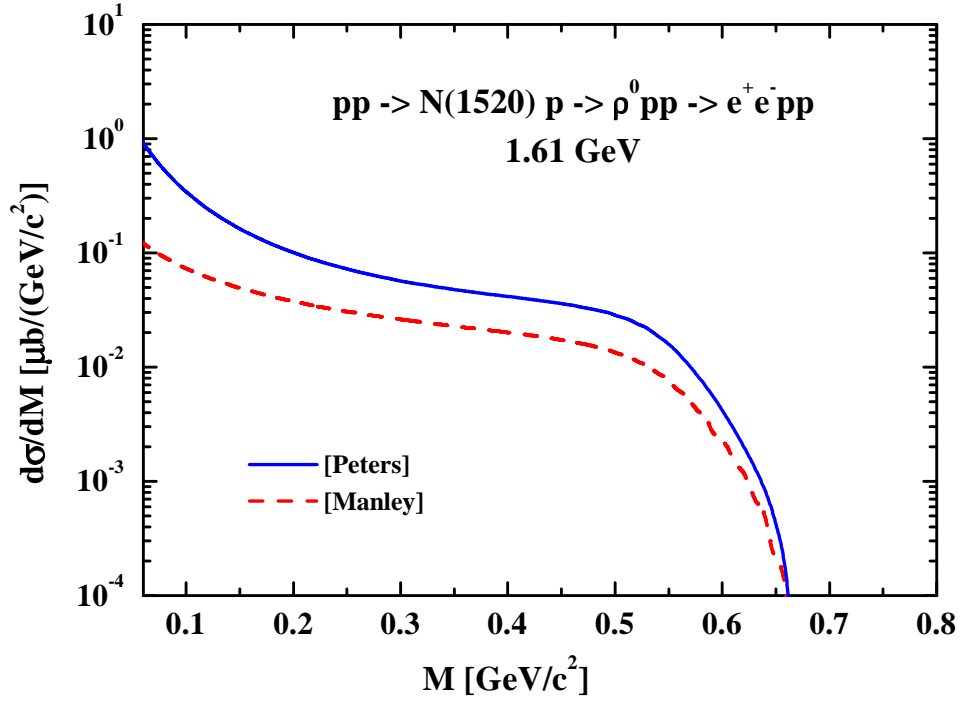


FIG. 3. The dilepton invariant mass spectra from the channel $pp \rightarrow N(1520)p \rightarrow \rho^0 pp \rightarrow e^+e^-pp$ at 1.61 GeV calculated according to the resonance model of Peters et al. [14] (solid line) and Manley et al. [41] (dashed line) without implementing an experimental filter.

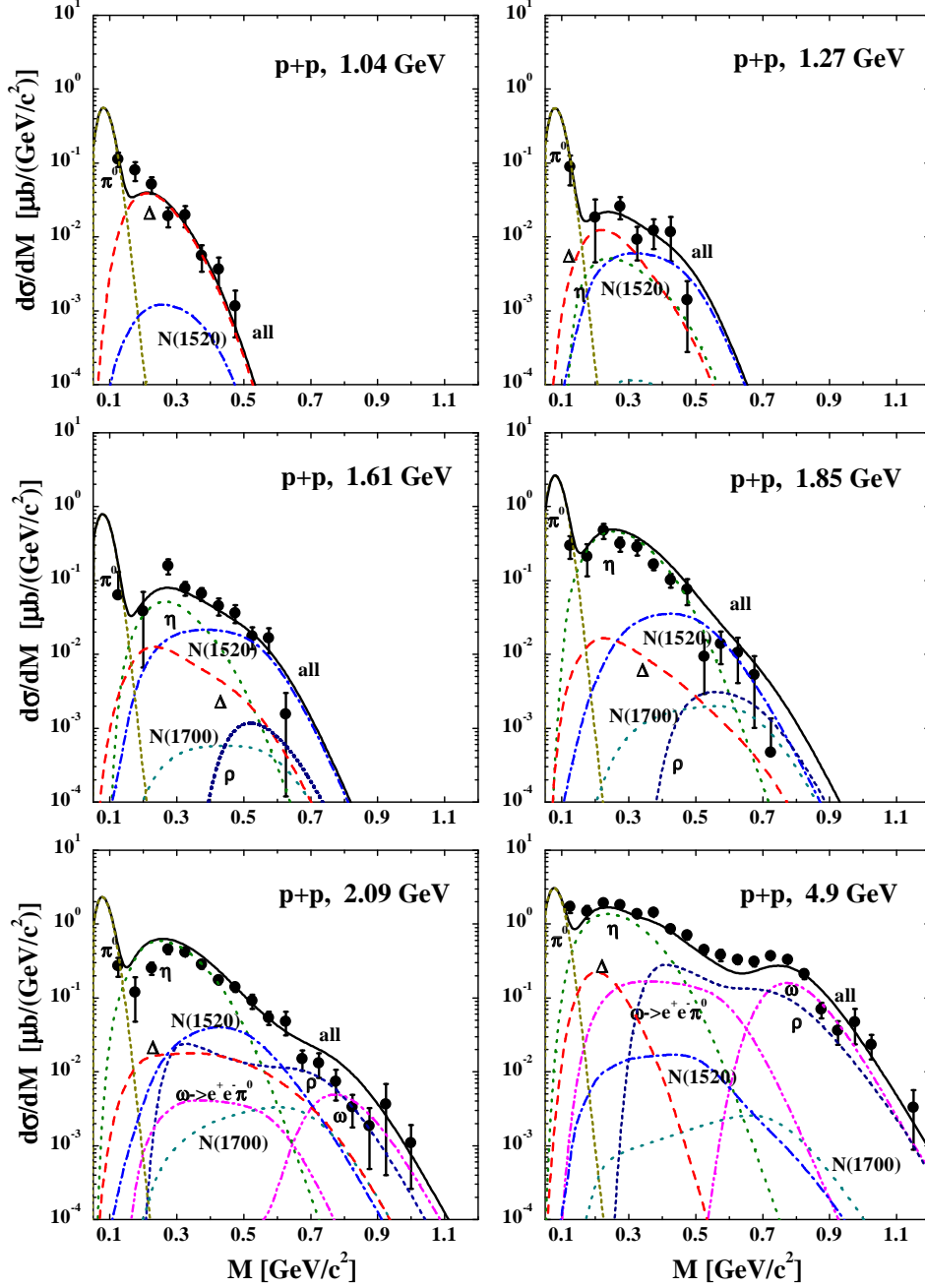


FIG. 4. The calculated dilepton invariant mass spectra $d\sigma/dM$ for pp collisions from 1.0 – 4.9 GeV in comparison to the DLS data [32]. The thin lines indicate the individual contributions from the different production channels; *i.e.* starting from low M : Dalitz decay $\pi^0 \rightarrow \gamma e^+ e^-$ (short dashed line), $\eta \rightarrow \gamma e^+ e^-$ (dotted line), $\Delta \rightarrow N e^+ e^-$ (dashed line), $\omega \rightarrow \pi^0 e^+ e^-$ (dot-dot-dashed line), $N(1520) \rightarrow N e^+ e^-$ (dot-dashed line); $N(1700) \rightarrow N e^+ e^-$ (dotted line); for $M \approx 0.7$ GeV: $\omega \rightarrow e^+ e^-$ (dot-dot-dashed line), $\rho^0 \rightarrow e^+ e^-$ (short dashed line). The full solid line represents the sum of all sources considered here.

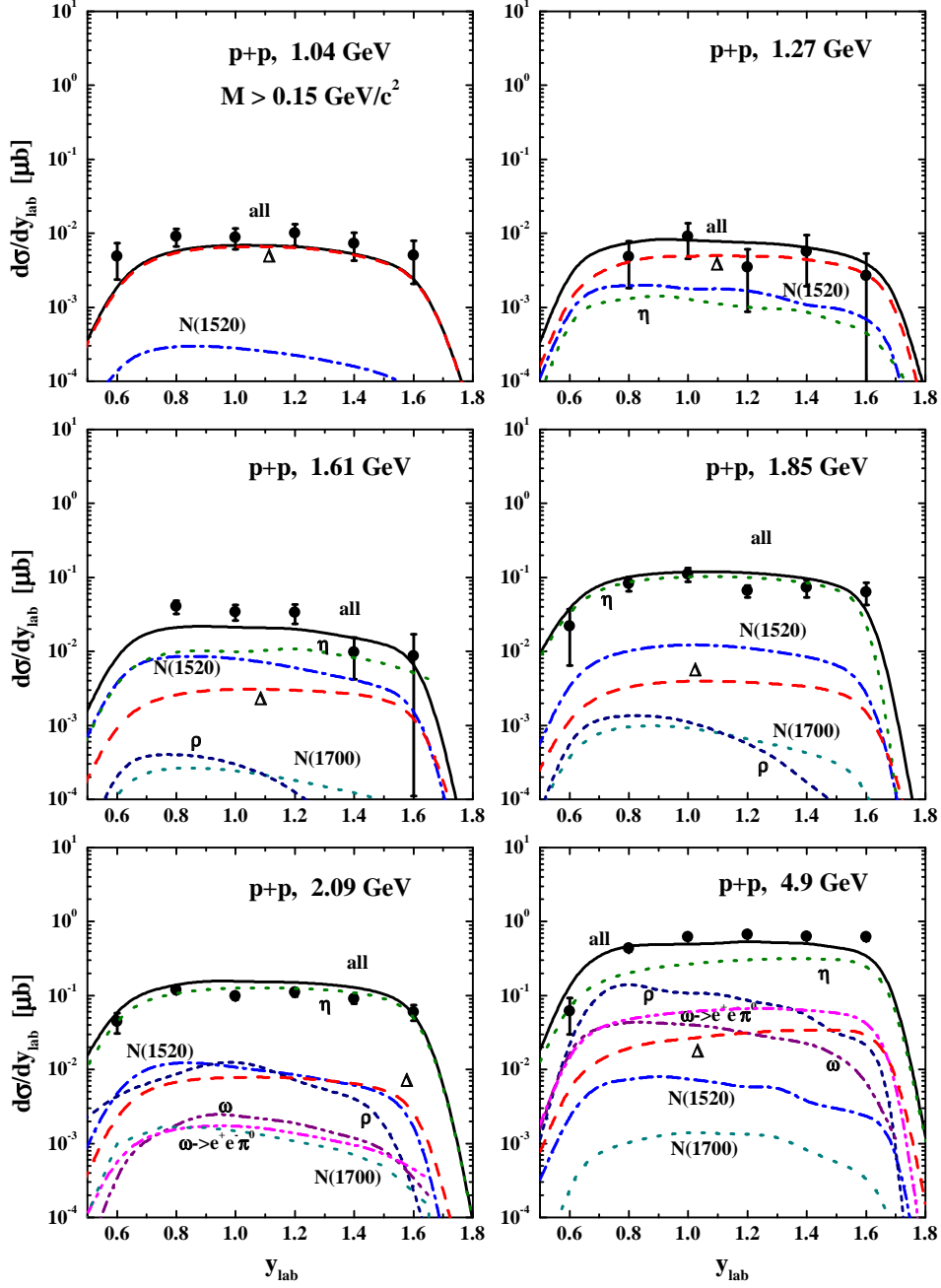


FIG. 5. The laboratory rapidity spectra of dileptons for pp collisions at 1.0 – 4.9 GeV in comparison to the DLS data [32] with a low mass cut of $0.15 \text{ GeV}/c^2$. The assignment of the lines is the same as in Fig. 4.

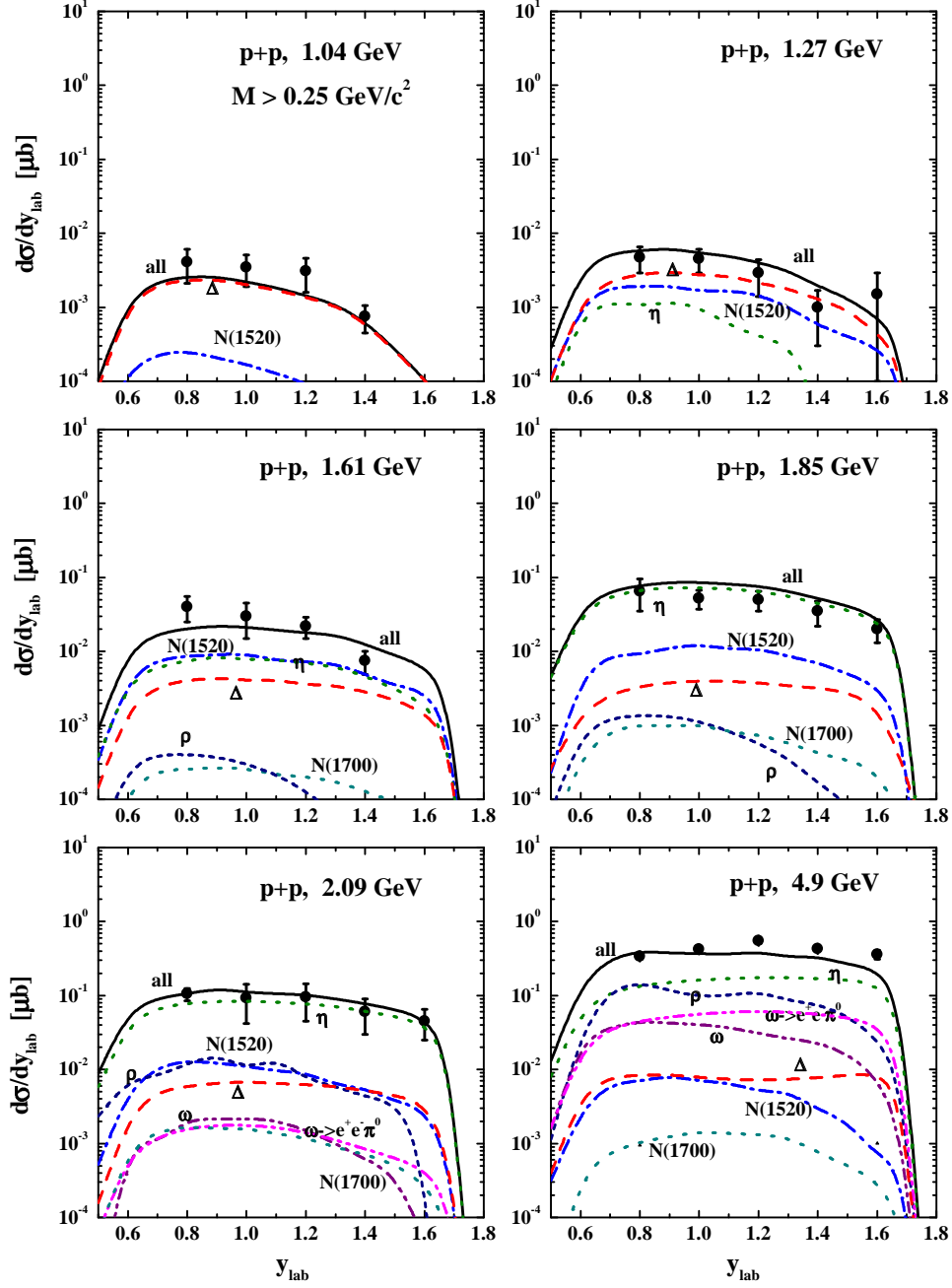


FIG. 6. The laboratory rapidity spectra of dileptons for pp collisions at 1.0 – 4.9 GeV in comparison to the DLS data [32] with a low mass cut of $0.25 \text{ GeV}/c^2$. The assignment of the lines is the same as in Fig. 4.

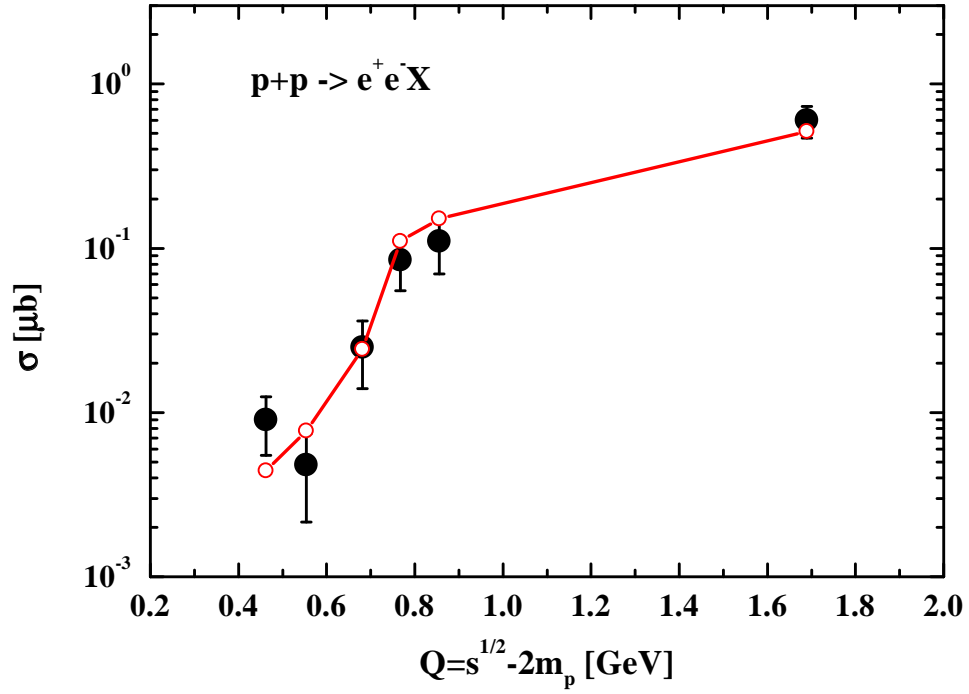


FIG. 7. The excitation function for dileptons from pp collisions for masses $M > 0.15 \text{ GeV}/c^2$ in comparison to the DLS data [32].